energies

MDPI

Article

Energy Flexibility Evaluation for Building Passive Thermal Storage Mass

Haiyang Yuan [1], Yongbao Chen [1,2,*], Alessandra Di Gangi [3] and Zhe Chen [2]

[1] School of Energy and Power Engineering, University of Shanghai for Science and Technology, Shanghai 200093, China
[2] Department of Building Environment and Energy Engineering, The Hong Kong Polytechnic University, Hong Kong, China
[3] Dipartimento di Ingegneria, Università degli Studi di Palermo, 90128 Palermo, Italy
* Correspondence: chenyongbao@usst.edu.cn

Abstract

This study proposes a systematic methodology to evaluate the energy flexibility and operational performance of air-conditioning systems (ACSs) in residential buildings, leveraging the passive thermal storage capacity of building thermal mass through indoor temperature setpoint adjustment. A comparative analysis was conducted between inverter-controlled and intermittent on-off air conditioners under a baseline indoor temperature of 24 °C. Two additional temperature setpoint scenarios (26 °C and 28 °C) were tested to quantify variations in the building's electricity consumption demand. To characterize the dynamic thermal response across different floor levels, ground-floor, middle-floor, and top-floor apartments were investigated in a three-story residential building, enabling a controlled, floor-level comparison under identical control logic and climatic conditions. Dymola simulation software was employed to model and calculate ACS energy consumption and energy flexibility under the three temperature setpoint conditions (24 °C, 26 °C, and 28 °C). Results indicate that a strategy of scheduled ACS shutdown and automatic restart, enabled by the thermal inertia capacity of building thermal mass, effectively enhances ACS energy flexibility. Specifically, adjusting the zone temperature setpoint reduced the total ACS load by approximately 40% in two hours of a demand response event. This temperature setpoint adjustment strategy demonstrates significant potential to mitigate grid peak-load demand without compromising indoor thermal comfort and requiring additional building retrofitting investments. The findings provide a technical basis for optimizing residential ACS operation and promoting demand-side management in power systems.

Keywords: passive thermal mass; energy flexibility; demand response; temperature resetting

Check for updates

Academic Editors: Antonio Gagliano and Francesco Nocera

Received: 15 January 2026
Revised: 9 February 2026
Accepted: 14 February 2026
Published: 16 February 2026

1. Introduction

Residential energy consumption accounted for 26.1% of total energy consumption. For energy consumption in residential buildings, heating contributed 63.6%, while cooling accounted for 0.4% in the EU. However, countries with a Mediterranean climate consume relatively less energy for heating. For example, Malta consumed 20.4%, Portugal 28.2%, and Cyprus 35.4%. On the other hand, Mediterranean countries were among the highest consumers of cooling energy, with Malta at 12.3% and Cyprus at 11.4%. For Malta, this represented a significant increase from the previous year, in which the consumption for cooling was at 8.3% [1]. Furthermore, these numbers are expected to rise over the next few years due to the influences of global warming.

Electricity covers all the energy requirements for cooling through air-conditioning systems (ACSs), while heating is provided via various energy sources, including renewables, oil, gas, and electricity. The increase in the average summer temperature causes a corresponding increase in electricity consumption. This increase can potentially lead to electricity disruptions, and may require power grid operators to add additional network infrastructure to support the new peak demands. However, these infrastructural investments can be delayed or avoided by incentivizing building demand response (DR) techniques. The DR at the residential level is an emerging strategy for peak demand reduction by allowing direct load control. DR aims to manage electricity demand through different strategies that directly affect the aggregated load profile daily or seasonally through the active participation of the end-users [2]. Several studies focused on the DR of residential ACSs have shown great potential in reducing the peak demand during the summer months [3,4].

Li et al. [5] investigated energy management strategies for zero-energy buildings by optimizing the flexible scheduling of distributed energy resources, including battery energy storage, heat pumps, and building thermal mass as a passive thermal energy storage system. Their results showed that coordinated demand-side management significantly increased photovoltaic self-consumption and reduced operational costs by more than 15%, highlighting that building thermal mass can effectively contribute to energy flexibility without requiring additional active storage devices. Yang et al. [6] analyzed the impact of integrated energy flexibility from building thermal mass and hot water storage tanks on heating system operation in a low-energy building connected to district heating. Using detailed Modelica-based simulations, they demonstrated that fully charged building thermal mass could maintain indoor thermal comfort for up to 43 h. The results showed that combining building mass with active thermal storage significantly enhanced flexibility potential and reduced daily heating costs by shifting peak loads to low-price periods.

Chen et al. [7] developed a robust chiller sequencing strategy using probabilistic cooling load prediction and adaptive thresholds. Their real-world implementation reduced daily chiller switching by 56.5% and improved system COP by 4.2%. Chen et al. [8] developed a physics-informed neural network (PINNs) model by integrating a simplified resistance–capacitance (2R2C) thermal model with a data-driven neural network, demonstrating improved accuracy in indoor temperature and load prediction compared to conventional approaches. ACS operation in buildings is crucial to DR [9]. In the field of building DR, shutting ACSs off temporarily and resetting the zone temperature during the grid peak load time are two common approaches. Beyond peak load reduction and energy shifting, recent studies have emphasized the potential of building HVAC systems to provide ancillary services to power systems through their inherent operational flexibility. The concept of grid-responsive buildings has been proposed to enable HVAC-driven demand response resources to support grid services, such as frequency regulation and reserve provision, while maintaining indoor comfort [10]. From a system perspective, demand response has increasingly been recognized as a viable ancillary service product, highlighting the strategic role of flexible building loads in future electricity markets [11].

Many studies have shown that these are efficient strategies to achieve load reduction [12,13]. The heating and cooling load can be shifted because of the heat inertia effect of building thermal mass [14]. Typically, indoor temperature setpoints can be reset to 26 °C instead of 24 °C during the cooling season to reduce the ACS's power consumption. Lind and Ottermo [15] evaluated the flexibility potential of buildings by exploiting thermal inertia through different heat emission systems. Using a validated TRNSYS simulation model for a multi-family residential building, they compared thermally activated building systems, embedded surface systems, and radiator systems under several DR scenarios.

Their results showed that thermally activated building systems exhibited the longest response time, the shortest recovery time, and the smallest indoor temperature variation, indicating superior flexibility performance. Salo et al. [16] investigated optimal DR control strategies for buildings connected to district heating networks from the operator perspective. Based on system-level simulations, they found that DR alone yielded limited cost reductions; however, the integration of hot water thermal storage significantly enhanced peak load balancing capability and improved the economic viability of DR strategies at the system scale.

In a previous experimental study, our work [17] concluded that resetting the zone temperature by 2 °C was effective for short-term (0.5 h) and intermediate-term (2 h) DR programs. Aduda et al. [18] concluded that a total load reduction of 25% with a continuous time of 20 min could be achieved by resetting the normal temperature setpoint to 2 °C during the summer season in an office building. Li et al. [19] evaluated the demand response potential of residential air conditioning systems through field measurements and multi-scenario simulations. By comparing different control strategies, including temperature setpoint adjustment and on/off cycling, they showed that setpoint adjustment provided effective load reduction while better maintaining occupant comfort. Malik et al. [3] analyzed the contribution of ACSs to the regional summer electricity demands in New South Wales, Australia. The air-conditioning energy profiles obtained across the households from Sydney, Australia were then characterized by a 'K-means' clustering approach. Residential ACSs showed significant DR potential, which reached 9.0% of the total peak demand in some districts. However, the households participating in the study were from a geographically limited area and ACS operation may differ in other regions with higher humidity and temperatures.

The temperature setpoint of the ACS is critical in determining the cooling energy consumption of residential buildings and the degree of living comfort. Yan et al. [20] identified the typical temperature-setting patterns for ACSs by using big data measured from bedrooms and living rooms. The results showed that temperatures are typically set in the range of 24 °C to 26 °C and that setpoint selection has a direct effect on energy consumption. Yao [21] analyzed the effect of the random behavior of residents with standard cooling settings for central ACSs in a typical apartment in Ningbo, China. The models showed that standard settings overpredict the cooling load and result in non-optimal energy consumption. However, the model did not account for the diversity in residential behaviors, and no occupancy data were obtained for the development of the model. Xia et al. [22] also considered the effects of residential behavior and the ACS settings on energy consumption. However, the study was limited to bedrooms and relied on a small sample size. Young et al. [23] evaluated the reduction in peak power demand by regulating the building ventilation systems in commercial buildings. The results showed that up to 40% of the total peak load demand could be eliminated for a duration of 1.5 to 8 h under different building types and climates. Chen et al. [24] proposed a multi-objective optimization framework for online control, enhancing both smoothness and efficiency. Applied to chiller loading, it reduced equipment switching by 18.9% without compromising energy performance. Qi et al. [25] studied the DR potential of residential air conditioning loads and concluded that the ACS could be temporarily shut off without sacrificing the living comfort due to the thermal inertia of buildings. Dranka et al. [26] assessed that the peak load reduction potential in Brazil would increase from 12.8 GW to 25.6 GW by 2050. Furthermore, the authors also found that the residential sector holds the highest potential for peak load reduction.

Residential hybrid energy systems also provide the potential to deploy local DR, which could reduce overall energy consumption and reduce greenhouse gas emissions. Nizetic et al. [27] studied the hybrid energy strategy in the Mediterranean based on split air conditioning units. The authors proposed a hybrid energy system consisting of photovoltaics (PV), natural gas fuel cells, and split air conditioning units. Settino et al. [28] considered using the PV and heat pump in combination with batteries or thermal storage to allow for peak shaving, showing that local generation and storage can reshape the energy profile and reduce peak-hour consumption. However, the costs and space requirements associated with PV systems, fuel cell storage tanks, and thermal storage solutions limit their large-scale deployment in existing residential buildings.

Wang et al. [29] investigated the integration of phase change materials (PCMs) into building envelopes combined with intelligent control strategies to improve building energy flexibility. Using a verified numerical model and multi-objective optimization, they showed that PCM-integrated buildings could achieve flexibility index improvements of up to 32.78% and peak load reductions exceeding 90%. Nevertheless, such improvements often require design-stage interventions and advanced control strategies, which limit their applicability to existing residential buildings. Compared with material-intensive or hybrid solutions, DR strategies relying on existing building thermal mass and ACS control remain attractive due to their low cost and ease of deployment, especially for large-scale application in residential buildings.

This study aimed to investigate the effects of the ACS on energy consumption in residential buildings by isolating the role of passive building thermal mass under identical control conditions. The optimal temperature setpoint, which also ensures living comfort, was able to be determined. The building specifications, as well as the distribution of the flats, were also analyzed in this study, which focused on the determination of the thermal loads of the building with different physical characteristics. The size of the air conditioner was determined at steady states for each living room of the three flats located at the ground-level, intermediate-level, and upper-level of the building, allowing a controlled, floor-level comparison under the same climatic and operational assumptions. A simulation of the analyzed flats was built in the Dymola 2024x software for a typical summer day in July. Different operating conditions under various ACS setpoints were simulated.

2. Methodology

To systematically evaluate the energy flexibility of residential ACSs under different thermal conditions, a comprehensive energy analysis and modeling framework is developed. The methodology integrates steady-state thermal load calculation, dynamic building and system simulation, and scenario-based DR analysis. Three representative living rooms located on ground-level, intermediate-level, and upper-level flats of a residential building were modeled to ensure that differences in thermal behavior arise solely from vertical position and associated boundary conditions. The overall workflow consists of four main methodological steps: (i) determination of the cooling loads and selection of an appropriately sized inverter-controlled ACS, (ii) development of a detailed dynamic thermal model using the Modelica language on the Dymola platform, (iii) characterization of air conditioner performance under varying outdoor temperatures and part-load operation, and (iv) simulation of baseline and DR scenarios to quantify energy flexibility and energy savings. The building used in this study is a typical residential structure located in Palermo, Italy, built in the 1970s with a reinforced concrete frame. The study focuses on the living room of the flat, which has a total floor area of 7.16 m $\times$ 4.00 m and is equipped with two windows measuring 1.60 m $\times$ 2.00 m.

This integrated approach enables a consistent comparison of the thermal response and energy performance across different floor levels while accounting for building thermal mass, solar gains, and realistic air conditioner control behavior. By combining physicsbased thermal modeling with scenario-driven control strategies, the framework provides a robust basis for assessing the duration and magnitude of DR that can be achieved without significantly compromising indoor thermal comfort. Figure 1 illustrates the overall modeling and simulation framework adopted in this study, highlighting the main steps.

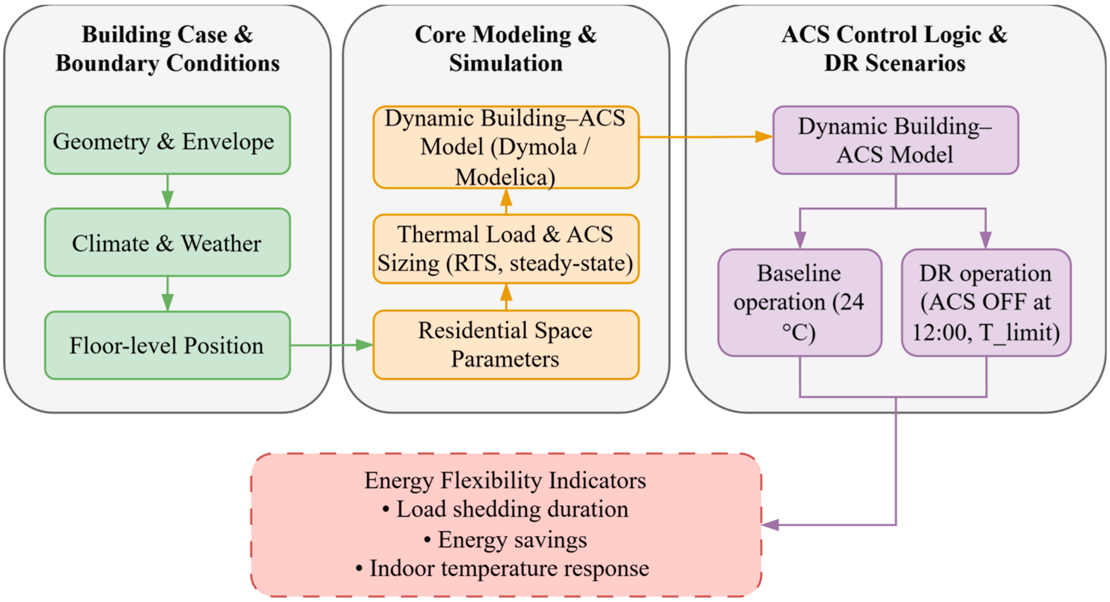

Figure 1. Methodology framework.

3. Building Case and Modeling

In this study, a typical residential building constructed in Palermo (Italy) in the 1970s was used. The building structure is characterized by a reinforced concrete frame, which represents the most common construction type for multi-story buildings in Palermo. The detailed building characteristics are listed in Table 1.

Table 1. Detailed building characteristics.

Building	Structure	Thickness (m)	Mass (kg/m^2)	Overall Heat Transfer Coefficient (W/m^2·K)	Density (kg/m^3)	Specific Heat (kJ/kg·K)
External wall	Plastered concrete hollow blocks	0.25	380.0	1.847	1520	0.837
Internal wall	Plastered concrete hollow blocks	0.12	186.9	2.544	1558	0.837
Floor	Hollow clay bricks reinforced by concrete beams covered by marble tiles	0.24	427.0	1.377	1780	0.880
Roof	Hollow clay bricks reinforced by concrete beams covered by ceramic tiles	0.24	427.0	1.644	1780	0.880
Window	Single glazed steel frame	-	-	7.010	-	-

Buildings constructed before the enforcement of modern energy efficiency regulations constitute a large share of the existing residential stock in Southern Europe. For such buildings, large-scale envelope retrofitting and the deployment of advanced energy storage systems are often constrained by economic and practical limitations. In this context, DR strategies that exploit the inherent thermal mass of existing structures provide a low-cost and scalable pathway to improve energy flexibility. Therefore, studying the DR potential of this building typology is particularly relevant for realistic grid integration scenarios. The typical flat of the building has a total area of 152 m^2 and includes a hall, a living room, three bedrooms, a kitchen, and two bathrooms, as shown in Figure 2. The study focused on the living room, as shown in Figure 3, which has a gross floor area of 7.16 $\times$ 4.00 m^2, and two windows of 1.60 $\times$ 2.00 m.

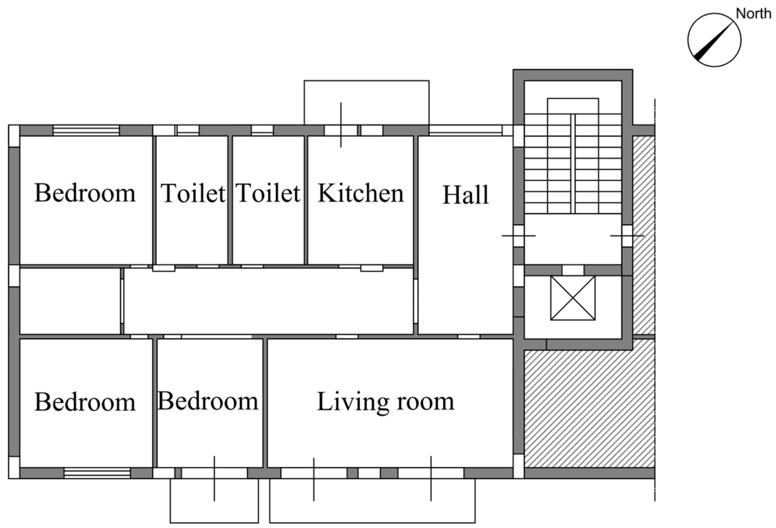

Figure 2. Flat layout of the building case.

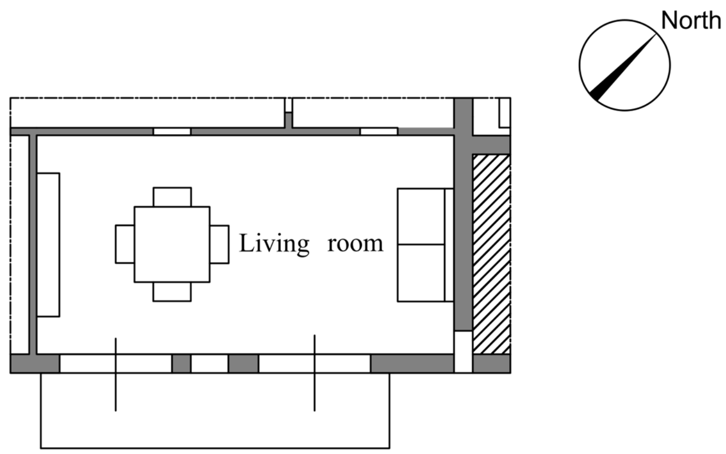

Figure 3. Floor plan of the living room.

The size of the air conditioner was determined at steady state conditions for each living room of the three flats located at the ground level, intermediate level, and upper level of the building. The outdoor temperature was assumed to be constant at 32 °C, while the indoor temperature was set to 26 °C. The Northeast–Southwest orientation was considered, with the living room facing southeast. According to the thermal load, which was calculated by considering the solar and indoor heat gains, two different types of air-to-air split system inverter-controlled air conditioners were selected. The selection of different ACS capacities reflects the realistic steady-state cooling demand of each flat, which varies with vertical position, solar exposure, and envelope boundary conditions. In particular, the upper-level flat requires a higher nominal cooling capacity due to additional heat gains from the roof, while the intermediate-level flat exhibits lower peak cooling demand. These differences in ACS sizing are therefore a consequence of building thermal characteristics rather than an independent control variable. To ensure comparability, all flats are subjected to identical control logic, temperature setpoint limits, and climatic conditions, and the assessment of energy flexibility focuses on relative energy reduction, interruption duration, and thermal response rather than absolute system capacity. The air conditioner performance at the rating conditions (outdoor air temperature 35 °C, indoor air temperature 26 °C) and at the minimum/maximum rotation speed of the ACS compressor are shown in Table 2 [30]. Performance is shown as Type A for the intermediate-level flat and Type B for ground- and upper-level flats.

Table 2. Characteristics of the ACSs at the rating conditions.

Air-Conditioner Model (Daikin)		Min	Rated	Max
Type A	Cooling capacity [kW]	1.40	3.50	4.00
FTXS35G2V1B	Power Input [kW]	0.35	0.87	1.19
RXS35G2V1B	Coefficient of performance	4.00	4.02	3.36
Type B	Cooling capacity [kW]	1.70	5.00	6.00
FTX50GV1B	Power Input [kW]	0.44	1.55	2.08
RX50G2V1	Coefficient of performance	3.86	3.23	2.88

To evaluate the COP at different operational conditions, such as different outdoor temperatures, different indoor temperatures, and different cooling capacities of the specific air conditioner, the cooling load of each room was calculated according to the radiant time series method described by ASHRAE [31]. This method is particularly suitable for buildings with high thermal mass, as it captures the time-delay effect between heat gains and cooling loads. The heat gains due to the solar energy through the windows, the inhabitants, the lights, the equipment, and the appliances were considered.

The data for outdoor air temperature and direct and diffuse solar radiation were obtained from the hourly data sets provided by the Astronomical Observatory of Palermo for the typical meteorological year [32]. The calculations were performed for each hour of the summer season, which includes June, July, August, and September. Figures 4–6 depict the variations in the thermal load for each flat level.

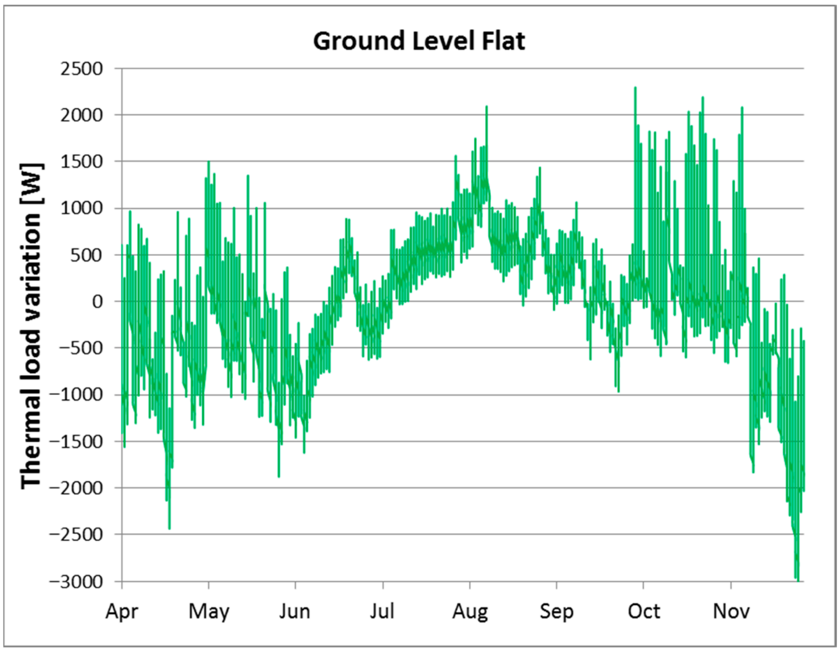

Figure 4. Thermal load variation for the ground-level flat.

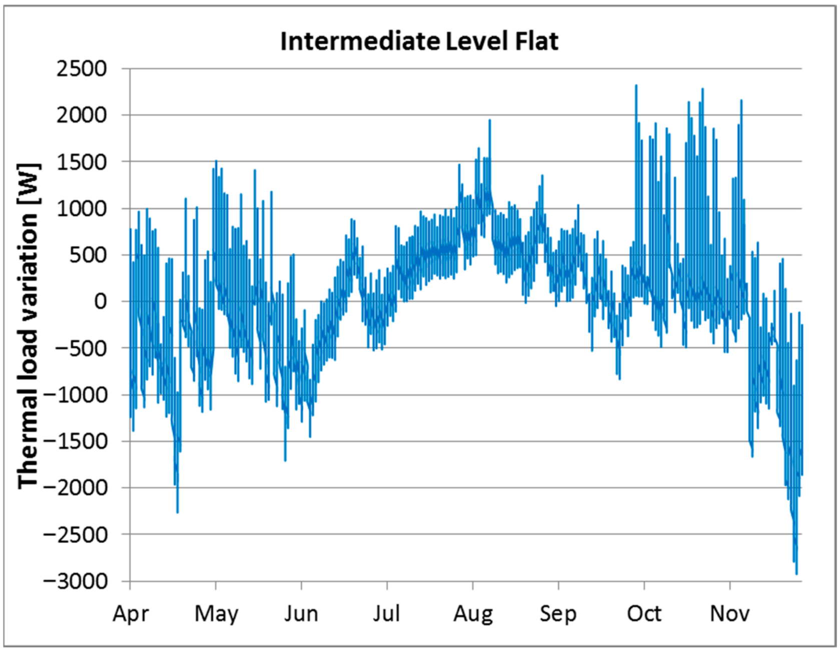

Figure 5. Thermal load variation for the intermediate-level flat.

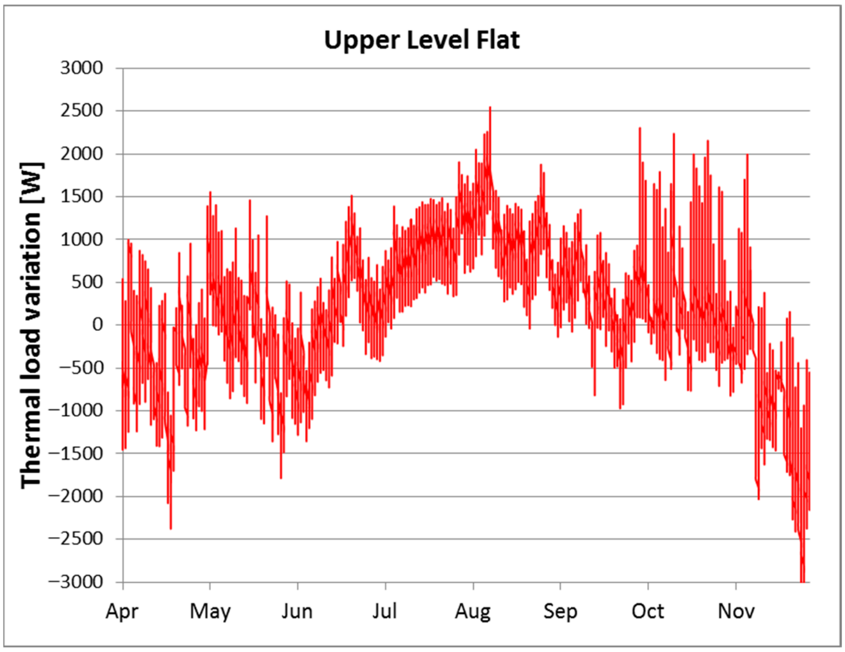

Figure 6. Thermal load variation for the upper-level flat.

The above is based on the linear interpolation of the data provided by the manufacturer for different outdoor temperatures at the indoor temperature of 26 °C, as shown in Table 3, which summarizes the manufacturer-provided performance characteristics of the selected ACS units under rating and part-load conditions. This approach allows the performance variation of inverter-controlled ACS units to be represented in a simplified yet physically consistent manner, without introducing additional empirical fitting parameters. The calculated nominal value of COP was used to evaluate the COP at the current compressor speed rotation related to the cooling capacity of the ACS. Accordingly, a parabolic interpolation between the calculated nominal COP and the COP at the minimum/maximum rotation speed was adopted. Thus, the same proportion between the nominal COP, the minimum COP, and the maximum COP, as listed in Table 3, was maintained.

Table 3. ACS performance under part-load and rating conditions.

Air-Conditioner Model (DAIKIN)		Outdoor Air Temperature					
		20 °C	**25 °C**	**30 °C**	**32 °C**	**35 °C**	**40 °C**
Intermediate-level Size C FTXS35G2V1B RXS35G2V1B	Cooling capacity (kW)	3.99	3.83	3.66	3.60	3.50	3.34
	Power Input (kW)	0.68	0.74	0.81	0.83	0.87	0.93
	COP	5.87	5.18	4.52	4.34	4.02	3.59
Ground-level and upper-level Size D FTX50GV1B RX50G2V1	Cooling capacity (kW)	5.70	5.47	5.23	5.14	5.00	4.77
	Power Input (kW)	1.21	1.32	1.44	1.48	1.55	1.66
	COP	4.71	4.14	3.63	3.47	3.23	2.87

The annual COP values are 5.027, 4.812, and 4.869 for the intermediate-level, ground-level, and upper-level flats, respectively. The Dymola software, which is based on the Modelica language [33,34], was used to analyze the dynamic behavior of the ACS. This Dymola system model consists of an ACS, an air handling unit (AHU), pipes, pumps, and valves. The AHU model consists of a typical air handler with a cooling coil, a variable-speed fan, and a water-side valve. This valve can be controlled to meet the required outlet air temperature setpoint. The main components and parameters in Dymola are listed in Table 4.

Table 4. Main components and parameter settings in Dymola.

Component	Model Based on	Main Parameters Setting
Heat pump	Buildings.Fluid. Chillers.Carnot_TEva	Nominal mass flow rate of evaporator = 0.12 kg/s evaporator leaving water temperature = 7 °C nominal evaporator heat flow rate = 4.3 kW
Living Room	Buildings.ThermalZones.Detailed.MixedAir	Based on Table 1 ACS opening schedule 00:00–12:00, 22:00–23:00 total internal heat gain = 8 W/m^2 lights load density = 2 W/m^2 equipment load density = 4 W/m^2
AHU	Buildings.Applications.DataCenters.ChillerCooled. Equipment.CoolingCoilHumidifyingHeating	Nominal mass flow rate of air = 0.5 kg/s
Pipe	Buildings.Fluid.Fixed Resistances.Pipe	Pipe length = 10 m pipe diameter = 0.03 m
Weather Bus	Buildings.BoundaryConditions.WeatherData.ReaderTMY3	Weather data in Palermo

The simulation was carried out for a typical hot summer day (14 July), using the weather data provided by EnergyPlus 24.2 software [35]. The room model is a thermal zone that assumes the air is completely mixed, and the heat transfer through the building envelope and the ACS is considered [34]. It is worth noting that the furniture has similar thermal transfer characteristics to the indoor wall. Hence, an indoor wall model using the effective-area method was considered in Dymola, an approach that has been adopted in recent studies to represent the contribution of internal furnishings to the effective thermal mass of residential zones without explicitly modeling each object [36]. The simulations were carried out by assuming an initial indoor temperature of 24 °C to evaluate the variation in indoor temperature and the corresponding avoided electricity consumption until the temperature increased to either 26 °C or 28 °C. Other additional parameters for the simulations are summarized in Table 5.

Table 5. Parameters used for simulations.

Item	Data	Notes
Simulation date	14-July	Temperature is about 34 °C
City location (weather data source)	Palermo	Weather data from Energyplus website
Total area of living room (m^2)	28.6	Upper-level, intermediate-level and ground-level
Room height (m)	2.9	
Total heat gain from people and equipment (W/m^2)	8	Total = 8 × 28.6 = 228.8
Person occupancy	All day	
Room temperature setting (°C)	24	
Building construction information	Table 1	
ACS On	0:00–12:00, 22:00–23:00	ACS shut off at 12:00
ACS COP	5.027	Intermediate-level
	4.812	Ground-level
	4.869	Upper-level
AC ventilation airflow rate (kg/s)	0.02	

4. Results and Discussion

The modeling approach adopted in this study is consistent with previously validated research on demand response strategies exploiting building thermal inertia. Chen et al. [14] developed and validated a Dymola-based framework to quantify electricity flexibility in office buildings, demonstrating that peak load reduction can be achieved through temperature setpoint adjustments and the utilization of building thermal mass without violating comfort constraints. In particular, the magnitude and temporal characteristics of load shifting reported in [14] are comparable to the flexibility levels observed in the present study under the 26–28 °C temperature reset scenarios. This consistency indicates that the thermal response behavior captured by the proposed model is physically reasonable and aligned with established findings in the literature. It should be noted that the present study focuses on a comparative analysis across different floors and thermal conditions rather than direct experimental validation. Nevertheless, the agreement with previously validated Dymola-based studies supports the credibility of the modeling framework and the robustness of the derived conclusions.

The variations in the indoor temperature for the ground-level flat, intermediate-level flat, and upper-level flat are shown in Figure 7a, Figure 7b, and Figure 7c, respectively. The ACS effectively regulates the indoor temperature at 24 °C until it is turned off at 12:00 pm. These temperature profiles provide direct insight into the dynamic thermal response of the apartments under identical control actions but different thermal boundary conditions. By observing how indoor temperature evolves once active cooling is suspended, it becomes possible to assess the effective thermal inertia of each flat and its ability to passively maintain thermal comfort during a demand response event. The ACS remained off until the indoor temperature increased to 26 °C or to 28 °C, respectively.

Due to the thermal gain of the building (solar gain and user activities), the temperature of 26 °C was reached after 1.4 h, 48 min, and 26 min for the ground-level flat, intermediate-level flat, and upper-level flat, respectively. The markedly different times required to reach the same temperature threshold reveal the strong influence of vertical position on the thermal behavior of the apartments. Although all flats share identical layouts, construction, and control settings, their exposure to external heat gains and thermal coupling conditions differs substantially. These factors govern the rate at which stored heat accumulates in the indoor environment once mechanical cooling is interrupted. From a physical perspective, this behavior can be interpreted in terms of effective thermal inertia, which reflects the combined effects of building thermal mass, solar exposure, and boundary interactions. A higher effective thermal inertia allows the indoor temperature to increase more slowly under identical thermal gains, thereby extending the duration over which cooling can be curtailed without exceeding comfort limits.

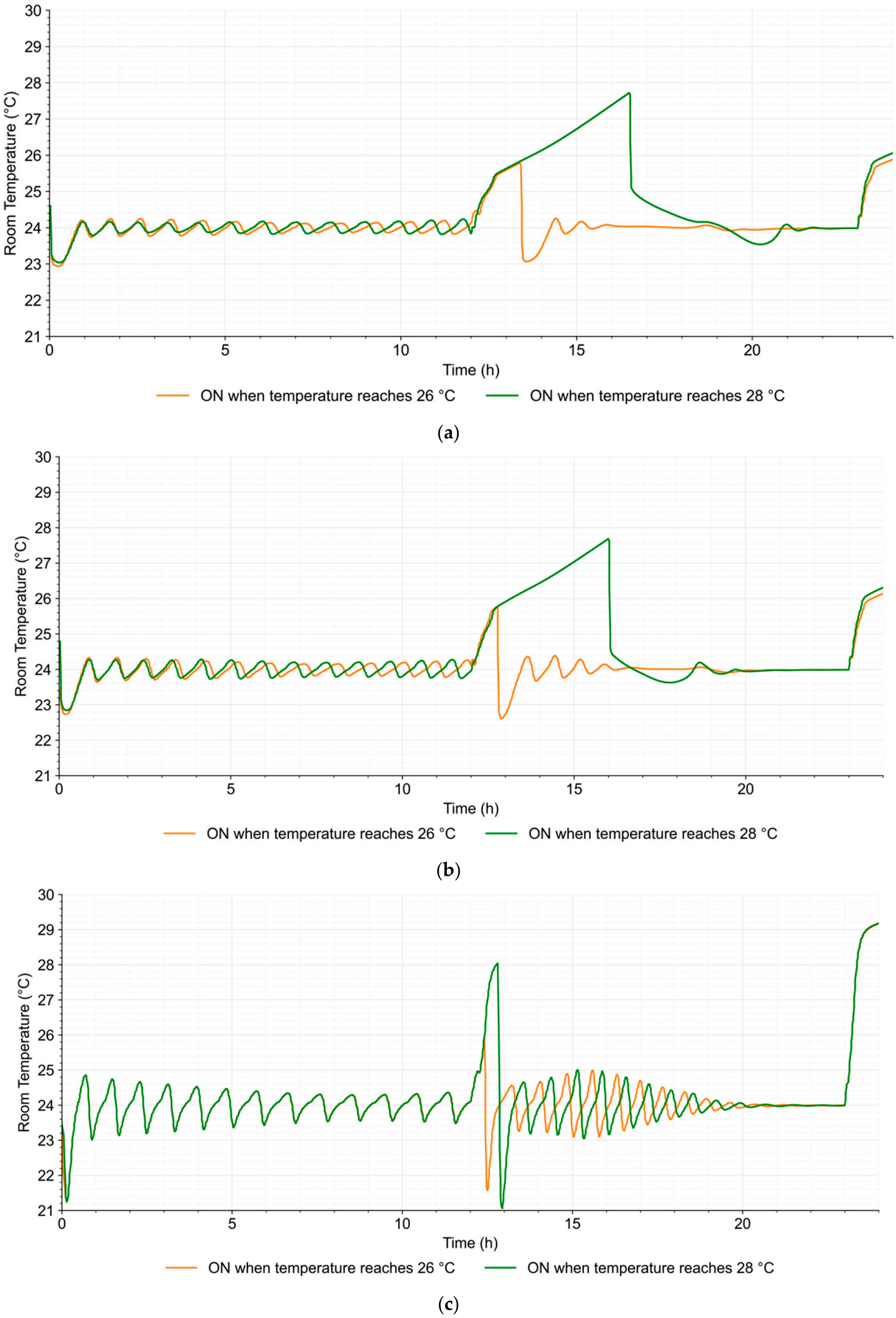

Figure 7. (**a**) Room temperature variations for the ground-level flat. (**b**) Room temperature variations for the intermediate-level flat. (**c**) Room temperature variations for the upper-level flat.

Comparing the two temperature limits further highlights how allowable comfort margins influence the duration of load shedding. While the 26 °C threshold represents a relatively conservative comfort constraint, increasing the limit to 28 °C significantly extends the off-time of the ACS, particularly for the ground-level and intermediate-level flats. This effect is not linear, indicating that the interaction between thermal gains and stored heat becomes increasingly dominant as the indoor temperature departs from the original setpoint. The contrast among the three flats becomes more pronounced at the higher temperature limit. For the upper-level flat, the rapid temperature rise results in a short interruption period even at 28 °C, whereas the ground-level flat can sustain several hours of passive temperature drift. This divergence suggests that identical control actions can lead to substantially different thermal outcomes depending on the apartment's position within the building.

The power consumption for the three flats is shown in Figure 8a–c. In addition to indoor temperature evolution, the electrical power demand of the ACS provides complementary information on how the system responds to shutdown and restart events. The instantaneous power profiles reflect not only the cooling load imposed by the outdoor conditions but also the system's effort to restore the indoor environment once operation resumes. For the ground-level flat, the peak power demand is 1.5 kW during both the 26 °C and 28 °C restart events. For the intermediate-level flat, the peak power demand is 1.43 kW during the 26 °C restart event, while it increases to 2.56 kW at the 28 °C limit. For the upper-level flat, the peak power demand is 1.43 kW during the 26 °C restart event, while it increases to 2.64 kW during the 28 °C restart event. The higher restart power observed in the intermediate-level and upper-level flats at the 28 °C limit indicates that a longer interruption period leads to greater accumulated thermal loads that must be removed once cooling resumes. As a result, the ACS operates closer to its maximum capacity during restart, producing a transient increase in electrical demand compared to normal operation earlier in the day.

The total energy consumption over a 24-h period is shown in Figure 9a–c. While the instantaneous power profiles illustrate the short-term response of the ACS to shutdown and restart events, the cumulative energy consumption over 24 h provides an integrated measure of the overall impact of the control strategy. This metric captures both the energy avoided during the interruption period and the additional energy required during restart, thereby offering a comprehensive basis for comparing the baseline and DR scenarios.

For the ground-level flat, the reference case showed a consumption of 14.6 kWh, while the consumption was only 7.81 kWh (−46.5%) and 6.43 kWh (−56%) at the setpoints of 26 °C and 28 °C, respectively. This substantial reduction in daily energy consumption reflects the strong ability of the ground-level flat to exploit thermal inertia. The long delay in temperature rise allows the ACS to remain off for extended periods, particularly in the 28 °C scenario, resulting in more than half of the baseline energy demand being avoided over the day. For the intermediate-level flat, the case showed a consumption of 13.6 kWh, while the consumption was only 7.09 kWh (−47.1%) and 6.1 kWh (−55.1%) at the setpoints of 26 °C and 28 °C, respectively. A similar trend is observed for the intermediate-level flat, with energy savings closely matching those of the ground-level flat in relative terms. Despite a shorter interruption period, the balanced thermal conditions of the intermediate floor enable effective load shifting while maintaining a comparable percentage reduction in daily energy use. In contrast, the upper-level flat exhibits a smaller reduction in total energy consumption. The rapid accumulation of heat following ACS shutdown leads to an earlier restart, limiting the duration of load shedding. Consequently, the achievable energy savings are lower, particularly when compared with the other two flats under the same control strategy.

https://doi.org/10.3390/en19041035

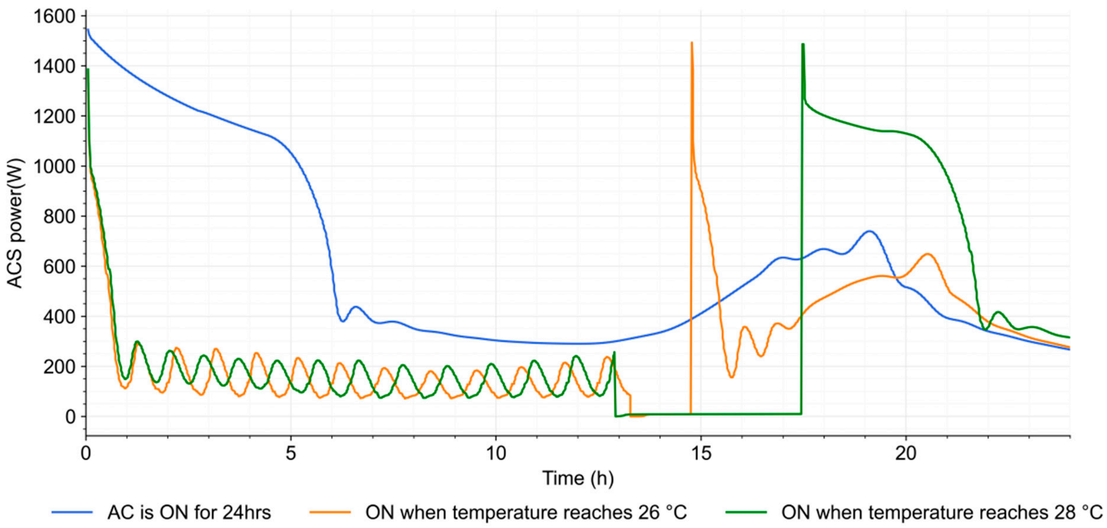

(**a**)

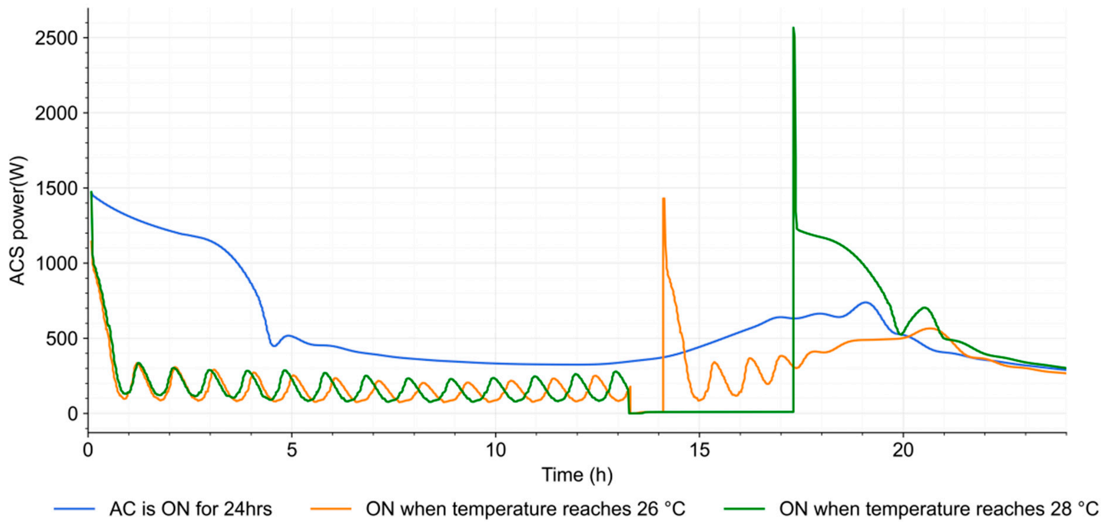

(**b**)

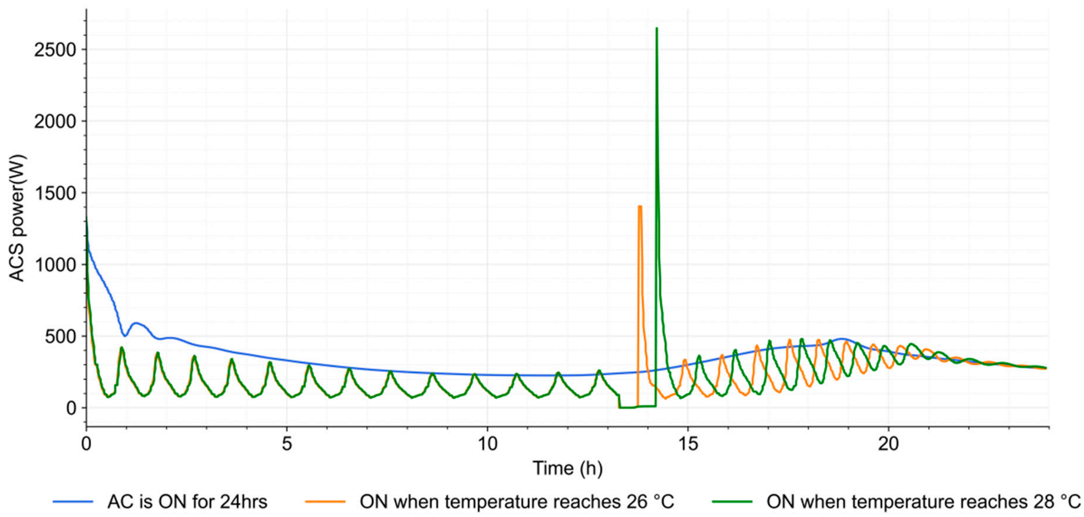

(**c**)

Figure 8. (**a**) Instantaneous power consumption for the ground-level flat. (**b**) Instantaneous power consumption for the intermediate-level flat. (**c**) Instantaneous power consumption for the upper-level flat.

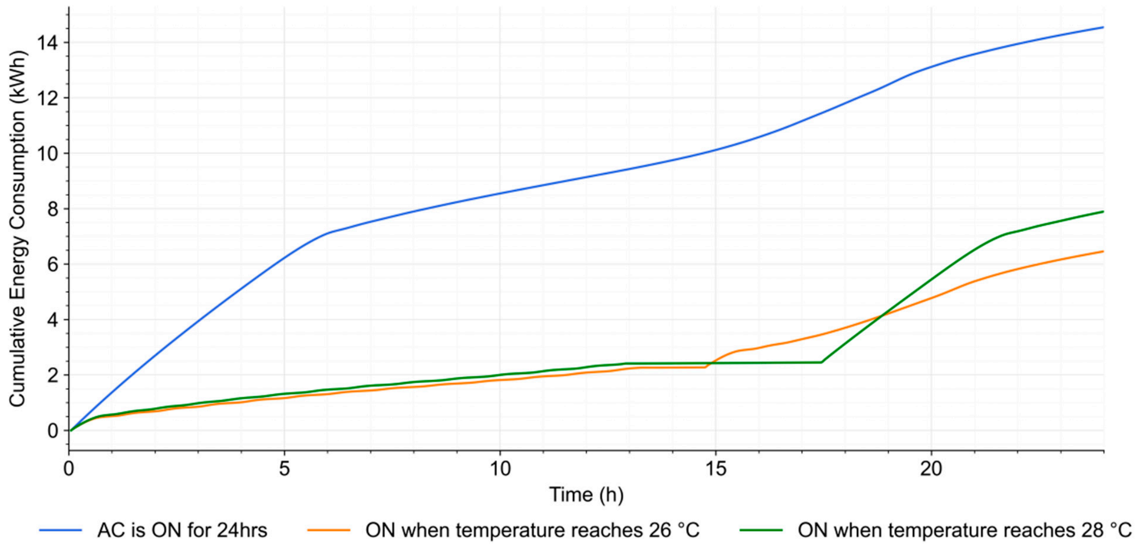

(**a**)

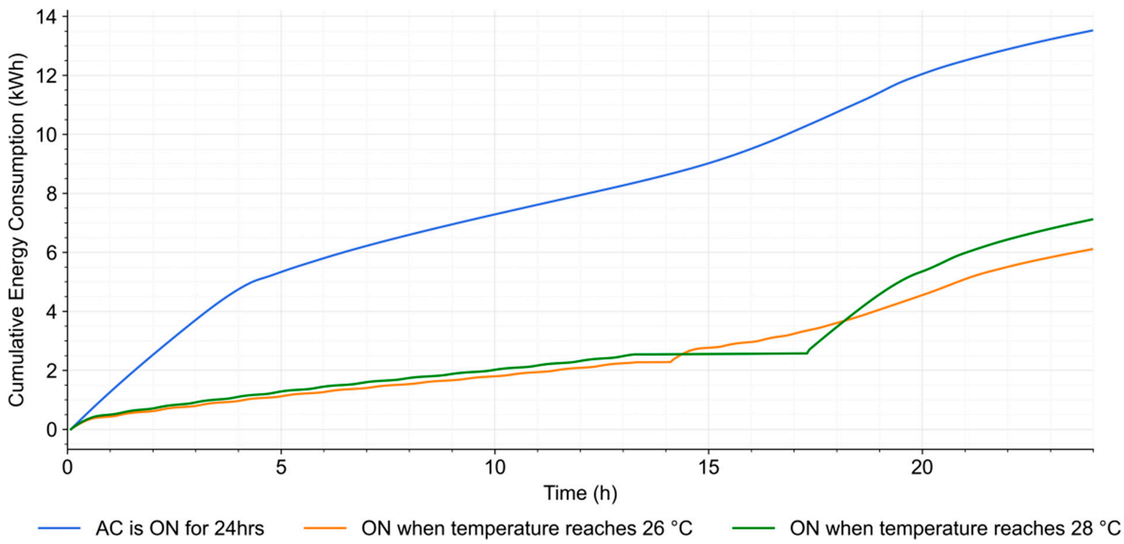

(**b**)

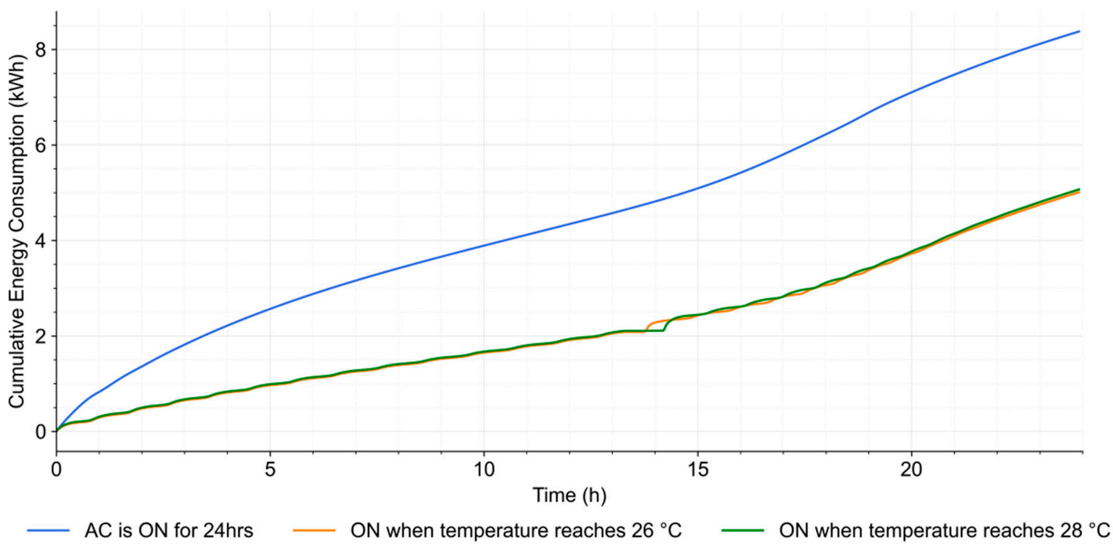

(**c**)

Figure 9. (**a**) Total energy consumption for the ground-level flat. (**b**) Total energy consumption for the intermediate-level flat. (**c**) Total energy consumption for the upper-level flat.

In addition to the reduction in total daily energy consumption, the restart behavior of the ACS after the DR event deserves further attention. When the ACS resumes operation after a prolonged shutdown, a transient increase in electrical power demand is observed, which reflects the accumulated cooling load that must be removed to restore the indoor temperature to the setpoint. This phenomenon is commonly referred to as the rebound effect.

To quantify this effect, the peak-to-baseline power ratio was evaluated for each flat and temperature limit. The peak power corresponds to the highest sustained power demand observed at the first regular simulation time step immediately after ACS restart, while the baseline power is defined as the ACS power at the same time instant under the "Always ON" reference condition. It should be noted that a very short-lived power spike appears at the exact moment of restart in the simulated power profiles. This spike is induced by numerical transients associated with the event-handling process of the dynamic solver and does not represent a physically sustained operating condition of the ACS. Therefore, the peak power reported in this study refers to the stabilized high-power level following restart that persists over a finite simulation interval, rather than the instantaneous numerical spike.

The results, summarized in Table 6, show that the rebound effect after ACS restart varies significantly across floor levels and temperature limits. For the upper-level flat, increasing the temperature limit from 26 °C to 28 °C leads to a pronounced increase in the peak-to-baseline ratio, from 5.63 to 6.58, indicating a strong rebound behavior after a prolonged shutdown period. This reflects the rapid heat accumulation and limited effective thermal inertia of the upper-level flat, which forces the ACS to operate close to its maximum capacity during recovery.

Table 6. Quantification of the rebound effect after ACS restart.

Flat Level	Setpoint 24 °C T_{limit}=	Peak Power (W)	Baseline Power (W)	Peak-to-Baseline Ratio
Upper-level	26 °C	1404.42	249.25	5.63
	28 °C	1734.57	263.52	6.58
Middle-level	26 °C	1119.13	375.76	2.98
	28 °C	1342.31	631.63	2.12
Ground-level	26 °C	1101.77	393.30	2.80
	28 °C	1323.14	634.44	2.08

For the intermediate-level and ground-level flats, the rebound behavior is more moderate. Although the absolute peak power increases when the temperature limit is raised to 28 °C, the corresponding baseline power under the "Always ON" condition also increases, resulting in lower peak-to-baseline ratios compared to the upper-level flat. In particular, the intermediate-level flat exhibits a decrease in the peak-to-baseline ratio from 2.98 to 2.12 when the temperature limit is increased from 26 °C to 28 °C, suggesting that the rebound severity is partially mitigated by its higher baseline cooling demand and more balanced thermal response.

In addition to peak power, the additional energy consumed during the recovery phase was also evaluated. Although part of the avoided energy during the DR period is offset by increased consumption after restart, the results indicate that the net daily energy savings remain substantial for all flats. Nevertheless, the rebound effect becomes more pronounced at higher temperature limits and for apartments with lower effective thermal inertia, particularly the upper-level flat.

From a grid perspective, these findings highlight the importance of coordinated or staggered restart strategies in large-scale DR deployment. As discussed in our previous work on smooth load reduction and recovery, the simultaneous restart of a large number of ACS units may lead to secondary peaks that partially undermine the benefits of peak load shedding. While such coordinated control strategies are beyond the scope of the present study, the quantified rebound indicators provided here offer a practical basis for incorporating smooth recovery constraints into future residential DR programs.

The results, summarized in Table 7, show that a scheduled turn-off ACS has the potential to reduce overall energy consumption, while it does not decrease the living comfort by much. It should be noted that the upper temperature limits of 26 °C and 28 °C considered in this study correspond to short-term demand response events rather than long-term indoor temperature settings. According to the adaptive thermal comfort framework defined in ASHRAE Standard 55 [31], higher indoor air temperatures can be acceptable for limited durations in naturally or mixed-mode residential buildings, particularly under Mediterranean summer conditions. Therefore, allowing the indoor temperature to temporarily drift up to 28 °C during controlled DR periods can be considered acceptable from a first-order comfort perspective, provided that the exposure duration is limited and the temperature is subsequently restored. The results also show the impacts of the flat level within the building (due to its thermal gain) and its ability to retain the setting temperature once the ACS is turned off. Table 7 consolidates the quantitative differences among the three flats and highlights the role of building position in shaping energy flexibility.

Table 7. Energy consumption comparison of different floors.

Flat	**Always ON**	**Setpoint 24 °C T_{limit} = 26 °C**	**Setpoint 24 °C T_{limit} = 28 °C**
		AC Turn-off at 12:00, 22:00–23:00 (Auto Turn-on When T_{actual} = T_{limit})	
Upper-level	8.41 kWh	5.18 kWh	5.07 kWh
Middle-level	13.6 kWh	7.09 kWh	6.10 kWh
Ground-level	14.6 kWh	7.81 kWh	6.43 kWh

It should be noted that the baseline energy consumption under the "Always ON" condition reflects not only the thermal load of the flat, but also the installed ACS's capacity and its operational characteristics. In this study, the upper-level flat is equipped with a higher-capacity ACS, which allows faster attainment of steady-state conditions and reduced operating time under continuous control. As a result, a lower baseline energy consumption does not necessarily indicate lower thermal gains, but rather a combined effect of building heat gains and system sizing. Therefore, the comparison of energy flexibility in this study is primarily based on relative load reduction and interruption duration under identical control logic, rather than on absolute baseline energy consumption alone. Although all apartments benefit from scheduled ACS shutdown, the magnitude of both energy savings and allowable interruption time varies significantly with floor level, driven by differences in thermal gains and heat dissipation pathways.

The upper-level flat reached the 26 °C and 28 °C limits earlier than the other two flats since it gains heat significantly faster. It resulted in a short ACS turn-off time and less energy saving. The temperature changing from the setpoint of 24 °C to the limit of 26 °C for the ground-level flat was an hour longer (about 3 times more) than that of the upper-level flat. The time difference for the temperature increased to 26 °C or to 28 °C was even more obvious. It clearly shows that different apartments within the same building have different potential for DR with temperature regulation. The time required for the indoor temperature to rise from the initial setpoint to the defined limits provides a clear temporal measure of flexibility. For the ground-level flat, the delay in reaching 26 °C is approximately three times longer than that of the upper-level flat, and the disparity becomes even more pronounced at the 28 °C threshold. This time-scale difference directly translates into different DR durations achievable under identical control actions. It is also worth noting that, in various instances, the ambient temperature may be below the indoor temperature, allowing the natural ventilation to improve living comfort and save additional energy. This observation suggests that temperature-based DR strategies could be further complemented by passive measures such as natural ventilation when outdoor conditions permit. Although not explicitly modeled in this study, the combined use of controlled ACS operation and passive cooling mechanisms may enhance both comfort and energy performance, particularly during transitional periods.

5. Conclusions

The capability of peak load reduction is important in the field of building DR and power grid integration. While temperature setpoint adjustment and ACS shutdown strategies have been widely investigated, the influence of apartment vertical location under identical control conditions remains insufficiently quantified. Therefore, a residential building located in Italy was investigated to provide a controlled, floor-level comparative assessment of energy flexibility driven by passive building thermal mass, supporting the integration of residential buildings into DR programs and energy demand management. This study considers the ground-level, intermediate-level, and upper-level flats as three different scenes to study the influence of different building thermal mass on room dynamic thermal characteristics. The main conclusions of this research are as follows.

- **Passive thermal mass serves as an effective, non-cost energy storage resource:** The thermal mass of building is an effective passive energy storage resource. Even though the ACS was turned off, the room temperature slowly increased from 24 °C to 28 °C after 4.5 h, 4 h, and 48 min for the ground-level flat, intermediate-level flat, and upper-level flat, respectively. This delay demonstrates the significant role of thermal inertia in maintaining indoor comfort during short-term load curtailment.
- **Intermittent ACS turn-off combined with temperature setpoint resetting is an effective short-term DR strategy:** The ACS intermittent turn-off strategy to regulate the room temperature can implement short-term DR programs of residential buildings in the hot and dry summer of the Mediterranean region. Allowing the indoor temperature to reset up to 26 °C or 28 °C enables meaningful peak load reduction during hot summer conditions in Mediterranean climates, while maintaining acceptable thermal comfort. In addition, this strategy leads to substantial reductions in daily cooling energy consumption during peak load periods.
- **Restart-related power rebound should be considered in large-scale DR deployment:** The ACS turn-off strategy has the potential for reducing energy consumption during the peak load times. A higher power demand was observed when the ACS restarted after longer interruption periods, particularly in the intermediate-level and upper-level flats. This rebound effect highlights the need for coordinated control strategies when applying temperature-based DR at scale, in order to avoid secondary load peaks. The rebound indicators reported in this study are derived from single-building simulations under fully synchronized restart assumptions and should therefore be interpreted as upper-bound estimates of post-DR peak impacts.

The potential for peak load reduction in the residential building is of crucial importance for the power grid. In future smart buildings, the building's electrical flexibility can be integrated with the energy supply of the power grid. Therefore, the future building's energy management will consider not only energy saving, but also energy flexibility. A building's energy system could respond to increases or decreases in load demand when the supply load of the power grid is overflowing or in shortage to maintain the balance of the power grid.

6. Future Work

This study is subject to several limitations. Simplified occupancy patterns and internal gains were assumed, and the analysis focused on a single building type in a Mediterranean climate. In addition, indoor air temperature was used as the primary indicator of thermal comfort. Future research should aim to achieve the following:

- **Incorporate more detailed comfort metrics**, such as operative temperature or adaptive comfort indices, to provide a more comprehensive assessment of thermal comfort during demand response events.
- **Validate the findings** through experimental studies or large-scale aggregation analyses, particularly to compare simulated temperature drift rates with real-world data and improve the robustness of the model.
- **Extend the analysis to other building types and climate conditions**, such as high-rise buildings, modern residential designs, and regions with different climatic conditions. These investigations would allow for a better understanding of how the proposed demand response strategies perform in diverse environmental and structural contexts.

Author Contributions: Conceptualization, H.Y. Yuan; methodology and manuscript writing, H.Y. and Y.C. Chen; formal analysis, A.D.G. and Z.C. All authors have read and agreed to the published version of the manuscript.

Funding: This research was supported by the National Natural Science Foundation of China (Grant No. 52208116) and the Shanghai Magnolia Talent Plan Pujiang Project (Grant No. 25PJD088).

Data Availability Statement: The original contributions presented in this study are included in the article. Further inquiries can be directed to the corresponding author.

Conflicts of Interest: The authors declare no conflict of interest.

References

1. Eurostat. *Energy Consumption in Households*; Eurostat: Kirchberg, Luxembourg, 2020.
2. Lampropoulos, I.; Kling, W.L.; Ribeiro, P.F.; van den Berg, J. History of demand side management and classification of demand response control schemes. In Proceedings of the 2013 IEEE Power & Energy Society General Meeting, Vancouver, BC, Canada, 21–25 July 2013.
3. Malik, A.; Haghdadi, N.; MacGill, I.; Ravishankar, J. Appliance level data analysis of summer demand reduction potential from residential air conditioner control. *Appl. Energy* **2019**, *235*, 776–785. [CrossRef]
4. Ruddell, B.L.; Salamanca, F.; Mahalov, A. Reducing a semiarid city's peak electrical demand using distributed cold thermal energy storage. *Appl. Energy* **2014**, *134*, 35–44. [CrossRef]
5. Li, Y.; Zhang, X.; Xiao, F.; Gao, W.; Liu, Y. Modeling and management performances of distributed energy resource for demand flexibility in Japanese zero energy house. *Build. Simul.* **2023**, *16*, 2177–2192. [CrossRef]
6. Yang, X.; Pan, L.; Guan, W.; Ma, H.; Zhang, C. Heat flexibility evaluation and multi-objective optimized control of a low-energy building with district heating. *Energy Build.* **2022**, *277*, 112523. [CrossRef]
7. Chen, Z.; Zhang, J.; Xiao, F.; Xu, K.; Chen, Y. Development of a probabilistic cooling load prediction-based robust chiller sequencing strategy and its real-world implementation. *Appl. Energy* **2025**, *382*, 125213. [CrossRef]
8. Chen, Y.; Wang, H.; Chen, Z. Sensitivity analysis of physical regularization in physics-informed neural networks (PINNs) of building thermal modeling. *Build. Environ.* **2025**, *273*, 112693. [CrossRef]
9. Pallonetto, F.; De Rosa, M.; Ettorre, F.D.; Finn, D.P. On the assessment and control optimisation of demand response programs in residential buildings. *Renew. Sustain. Energy Rev.* **2020**, *127*, 5–10. [CrossRef]
10. Wang, S.; Wang, J.; Tang, R. Grid-responsive buildings: A review of HVAC flexibility and demand response for power system support. *Appl. Energy* **2019**, *247*, 546–560.

11. Ribó-Pérez, D.; Peñalvo-López, E.; Pérez-Navarro, Á. Demand response products for ancillary services: A critical review. *Energies* **2021**, *14*, 846. [CrossRef]
12. Xu, P.; Haves, P.; Piette, M.A.; James, B. Peak demand reduction from pre-cooling with zone temperature reset in an office building. *Lawrence Berkeley Natl. Lab.* **2006**, *14*, 83–89.
13. Lee, K.; Braun, J.E. Development of methods for determining demand- limiting setpoint trajectories in buildings using short-term measurements. *Build. Environ.* **2008**, *43*, 1755–1768. [CrossRef]
14. Chen, Y.; Chen, Z.; Xu, P.; Li, W.; Sha, H.; Yang, Z. Quantification of electricity flexibility in demand response: Office building case study. *Energy* **2019**, *188*, 116054. [CrossRef]
15. Lind, J.; Ottermo, F. Energy flexibility in multi-family houses heated by thermally activated building systems. *Energy Build.* **2025**, *330*, 115345. [CrossRef]
16. Salo, S.; Hast, A.; Jokisalo, J.; Kosonen, R.; Syri, S.; Hirvonen, J.; Martin, K. The impact of optimal demand response control and thermal energy storage on a district heating system. *Energies* **2019**, *12*, 1678. [CrossRef]
17. Chen, Y.; Xu, P.; Chen, Z.; Wang, H.; Sha, H.; Ji, Y.; Zhang, Y.; Dou, Q.; Wang, S. Experimental investigation of demand response potential of buildings: Combined passive thermal mass and active storage. *Appl. Energy* **2020**, *280*, 159–178. [CrossRef]
18. Aduda, K.O.; Labeodan, T.; Zeiler, W.; Boxem, G.; Zhao, Z. Demand side flexibility: Potentials and building performance implications. *Sustain. Cities Soc.* **2016**, *22*, 146–163. [CrossRef]
19. Li, W.; Sui, W.; Cheng, L.; Ji, Y.; Guo, Y.; Zhu, J. Quantifying seasonal demand-side flexibility in residential air conditioning under diverse control strategies. *Energy Build.* **2026**, *352*, 116764. [CrossRef]
20. Yan, L.; Liu, M.; Xue, K.; Zhang, Z. A study on temperature-setting behavior for room air conditioners based on big data. *J. Build. Eng.* **2020**, *30*, 101197. [CrossRef]
21. Yao, J. Modelling and simulating occupant behaviour on air conditioning in residential buildings. *Energy Build.* **2018**, *175*, 1–10. [CrossRef]
22. Xia, D.; Lou, S.; Huang, Y.; Zhao, Y.; Li, D.H.; Zhou, X. A study on occupant behavior related to air-conditioning usage in residential buildings. *Energy Build.* **2019**, *203*, 35–47. [CrossRef]
23. Young, M.; Less, B.D.; Dutton, S.M.; Walker, I.S.; Sherman, M.H.; Clark, J.D. Assessment of peak power demand reduction available via modulation of building ventilation systems. *Energy Build.* **2020**, *214*, 134–152. [CrossRef]
24. Chen, Z.; Xiao, F.; Chen, Y. Multi-objective online optimization of building energy systems for improved control smoothness and efficiency. *Autom. Constr.* **2026**, *181*, 106604. [CrossRef]
25. Qi, N.; Cheng, L.; Xu, H.; Wu, K.; Li, X.; Wang, Y.; Liu, R. Smart meter data-driven evaluation of operational demand response potential of residential air conditioning loads. *Appl. Energy* **2020**, *279*, 153–178. [CrossRef]
26. Dranka, G.G.; Ferreira, P. Load flexibility potential across residential, commercial and industrial sectors in Brazil. *Energy* **2020**, *201*, 117483. [CrossRef]
27. Nizetic, S.; Papadopoulos, A.M.; Tina, G.M.; Rosa-Clot, M. Hybrid energy scenarios for residential applications based on the heat pump split air-conditioning units for operation in the Mediterranean climate conditions. *Energy Build.* **2017**, *140*, 110–120. [CrossRef]
28. Settino, J.; Sant, T.; Micallef, C.; Farrugia, M.; Staines, C.S.; Licari, J.; Micallef, A. Overview of solar technologies for electricity, heating and cooling production. *Renew. Sustain. Energy Rev.* **2018**, *90*, 892–909. [CrossRef]
29. Wang, P.; Liu, Z.; Liu, R.; Zhang, F.; Zhang, L. Design and operation control in multi-objective optimization considering phase change material. *Energy* **2023**, *268*, 126753. [CrossRef]
30. Daikin RXS-G2V1B Technical Data Manual, Daikin Europe N.V., Belgium, 2009. Available online: http://www.daikintech.co.uk/Data/Split-Sky-Air-Outdoor/RXS/2010/RXS-G2V1B/RXS-G2V1B_Databook.pdf (accessed on 16 December 2025).
31. *ASHRAE Handbook—Fundamentals*; ASHRAE: Atlanta, GA, USA, 2013.
32. Osservatorio Astronomico di Palermo. Available online: http://www.astropa.inaf.it/ (accessed on 16 December 2025).
33. *Open Source Library for Building Energy and Control Systems*; Lawrence Berkeley National Laboratory: Berkeley, CA, USA, 2018. Available online: http://simulationresearch.lbl.gov/modelica/index.html (accessed on 16 December 2025).
34. Wetter, M.; Zuo, W.; Nouidui, T.S. Modelica of heat transfer in rooms in the Modelica Buildings library. In Proceedings of the 12th Conference of International Building Performance Simulation Association, Sydney, Australia, 14–16 November 2011; pp. 14–16.
35. EnergyPlus Weather Data. Available online: https://energyplus.net/weather (accessed on 31 December 2025).
36. Qi, X.; Zhang, Y.; Liu, Z.; Wang, R. Quantifying the contribution of internal thermal mass to building energy flexibility: Implications for demand response modeling. *Carbon Neutrality* **2025**, *4*, 22. [CrossRef]